Plasmonics (2016) 11:45–51
DOI 10.1007/s11468-015-0016-1

Microfluidic Plasmonic Biosensor for Breast Cancer Antigen Detection

Johny Paulo Monteiro[1,3] · **Jean Halison de Oliveira**[1] · **Eduardo Radovanovic**[1] · **Alexandre Guimarães Brolo**[2] · **Emerson Marcelo Girotto**[1]

Received: 26 March 2015 / Accepted: 30 June 2015 / Published online: 11 July 2015
© Springer Science+Business Media New York 2015

Abstract Biosensors based on surface plasmon resonance (SPR), operating with the Kretschmann conventional arrangement, have been employed for biomolecular detection of tumor markers. However, the traditional SPR configuration presents some experimental inconveniences that are overcome by using plasmonic substrates based on nanohole arrays manufactured in metallic films. This SPR configuration exhibits the extraordinary optical transmission (EOT) phenomenon, which is explored in the monitoring of binding events that occur on the metal surface. In this work, we proposed a plasmon biosensor based on nanohole arrays built on gold film operating in collinear transmission mode by using spectral investigation for signal transduction. The SPR substrate was coupled to a microfluidic system and showed good sensitivity and linearity. A concentration of 30 ng mL^{-1} of human epidermal receptor protein-2 (HER2) antigen (associated with breast cancer) was detected using the integrated device; this showed its great potential to be used in tumor diagnosis.

Keywords Nanohole arrays · Surface plasmon · SPR · HER2 antigen · Tumor marker · Breast cancer

✉ Johny Paulo Monteiro
johnymonteiro@utfpr.edu.br

[1] Materials Chemistry and Sensors Laboratories, Department of Chemistry, State University of Maringá, Av Colombo 5790, 87020-900 Maringá, PR, Brazil

[2] Department of Chemistry, University of Victoria, P.O. Box 3065, V8W 3 V6 Victoria, British Columbia, Canada

[3] Present address: Department of Chemistry, Universidade Tecnológica Federal do Paraná - UTFPR, Marcílio Dias Street, 635, 86812-460 Apucarana, PR, Brazil

Introduction

The extraordinary optical transmission (EOT) through subwavelength nanoholes built on thin films of gold and silver was first reported by Ebbesen and coauthors in 1998 [1]. They observed a greater light transmission than what was predicted by the classical theory of Bethe on light diffraction through holes with dimensions of the order of the light wavelength [2]. The EOT is related to the surface plasmon resonance (SPR) excitation, which involves trapped light waves on the metal surface due to oscillation in resonance with electrons of the metal conduction band [1, 3]. The SPR phenomenon is highly sensitive to variations in the refractive index on the metal surface that supports surface plasmons (SPs). Therefore, plasmonic devices based on nanohole arrays constructed on gold films have been used to investigate binding events that occur on the metal surface in affinity biosensors while performing optical measurement [4, 5]. A SPR affinity sensor is characterized by a recognition element (immobilized on metal) that can recognize and interact with a specific analyte of a sample that is in contact with the metallic surface of transducer; this, in turn, converts the event binding in a measurable optical signal [3]. These sensors usually evaluate the band wavelength shift of the transmission spectrum in response to the molecular recognition of the analyte [4–6]. However, an investigation of changes in transmitted light intensity can also be employed [7, 8].

Traditional SPR biosensors based on the Kretschmann configuration require a prism attached to a thin metal film for excitation of SPs [9]. This type of sensor has been employed in various bioassays that range from the detection of analytes related to food quality and increased safety [10–14] to environmental monitoring [15–21]. This type of sensor has also been used for medical diagnosis regarding the detection of drugs [22–24], hormones [25–27], and markers for cancer

[28–35]. Despite the wide application and high sensitivity of the conventional SPR configuration, these devices have difficulty of setup alignment, which is a great experimental inconvenience [36]. Furthermore, these devices are not compact, which is an inconvenient feature that limits their application to field analysis and the degree of multiplexing. On the other hand, nanohole array-based plasmonic sensors overcome these experimental drawbacks. There is the possibility of operating in collinear optical arrangements with minimal sensory areas, which facilitate integration with microfluidic systems, multiplexing, and miniaturization [37, 38]. Nanohole array-based plasmonic biosensors built on gold thin films have been applied to biomolecular detection at various levels [4, 38–40].

The determination of tumor biomarkers is of great interest in medical diagnostics. These analytes are used to indicate the presence of cancer in patients, predict the behavior of a disease in response to treatment, predict the chance of patient recovery, and even help detect cancer in apparently healthy or high-risk people before the symptoms appear [41]. For instance, the detection of the paired box gene 8 (PAX8) protein, an important biomarker of ovarian cancer, has been reported by using nanohole array-based SPR biosensors on thin metallic films [39, 40].

Considering the advantages and applications of plasmonic biosensors based on nanostructured metallic films for traditional SPR devices, in this paper, we propose the detection of human epidermal receptor protein-2 (HER2), a cancer antigen, by using a biosensor based on a gold nanohole array integrated into a microfluidic system operating in spectral mode. The HER2 antigen is an important cancer marker that is in 20–25 % of individuals with breast cancer [42–45], and its determination is interesting since it is a marker that is used for the diagnosis and prognosis of the disease [45–47]. It is noteworthy that to our knowledge, the determination of this antigen by using SPR biosensors based on nanostructured gold film was not previously reported.

Experimental

Obtaining the Substrate Containing Nanohole Arrays

Square glass slides (2.5×2.5 cm and 1.0-mm thick) covered with 100-nm-thick gold films were used. A thin chromium layer (5-nm thick) was used as an adhesive layer between the glass and gold. These substrates were employed to obtain the nanohole arrays by a focused ion beam (FIB, FEI 235) with a dual-beam device by using a gallium ion source. The ion beam was set to 30 keV with a milling rate of 1.6 nm ms^{-1}, and the beam current was 300 nA. The diameter of each nanohole was 200 nm, and array periodicity was 400 nm. The substrates were characterized by scanning electron microscopy (SEM, Shimadzu Superscan SSX-550).

Microfluidic Chip

The microfluidic system was obtained by using well-established soft lithography techniques [48]. Square glass substrates (2.5×2.5 cm and 1.0-mm thick) were cleaned with acetone and piranha solution H_2SO_4 (FMaia, 95 %)/H_2O_2 (Anidrol, 35 %) in a 3:1 (*v*/*v*) ratio. Photomasks were created and printed on polyterephthalate sheets by using high-resolution printing. The photoresist (SU-8® 50, Microchem) was spin coated (Spincoating Systems, G3P-8) on a glass slide at 500 rpm for 5 s, dwelling for 8 s, ramping at 2000 rpm for 5 s, and spinning for 25 s. This resulted in a uniform thickness of ca. 50 μm. The coated glass slides were prebaked at 65 °C for 6 min and then at 95 °C for 20 min to harden the photoresist. The photomask was positioned on top of the photoresist film, and it was exposed under collimated UV light (Tamarack Scientific, 2110CP) for 17.5 s. The sample was then baked, first at 65 °C for 1 min and then at 95 °C for 5 min to promote cross-linking of the photoresist. The exposed glass slide was immersed in SU-8 developer until the unexposed photoresist was completely removed, which created the master templates. The microchannel structures were created by curing a solution of polydimethylsiloxane (PDMS, Sylgard 184®) and curing agent (Sylgard 184®) at a ratio of 10:1 *w*/*w* in order to create PDMS on the master templates. The PDMS was then degassed for 30 min in a vacuum and then cured at 95 °C for 2 h. The thickness of the PDMS was ca. 4.0 mm and microchannels with a width of 70 and 350 μm in spacing between channels.

Solution Flow and Optical Measurements

To obtain the transmission spectra, an experimental arrangement was used in a collinear mode, as shown in Fig. 1. This arrangement used a halogen lamp (300 W) with a broad emission band. The light was perpendicularly (normal) focused and collimated to the metallic nanohole arrays surface by using a ×50 objective lens (Meiji Techno, WD 7.5 mm) coupled to a trinocular microscope. The transmitted light was collected by an optical fiber (Ocean Optics, P600-2-UV-vis) positioned under the array. This optical cable was coupled to a UV-vis spectrophotometer (Ocean Optics, USB2000), and thus, transmission spectra were recorded and stored into a computer. The nanostructured metallic substrate was integrated with a microflow cell by using a PDMS piece that contained microchannels aligned to the array, as shown in the inset of Fig. 1. The flow of solutions was carried out with the aid of a syringe pump (Harvard Apparatus 11 Plus).

Sensor Sensitivity Characterization

The optical response of the sensor to changes in refractive index was performed by acquiring transmission spectra of

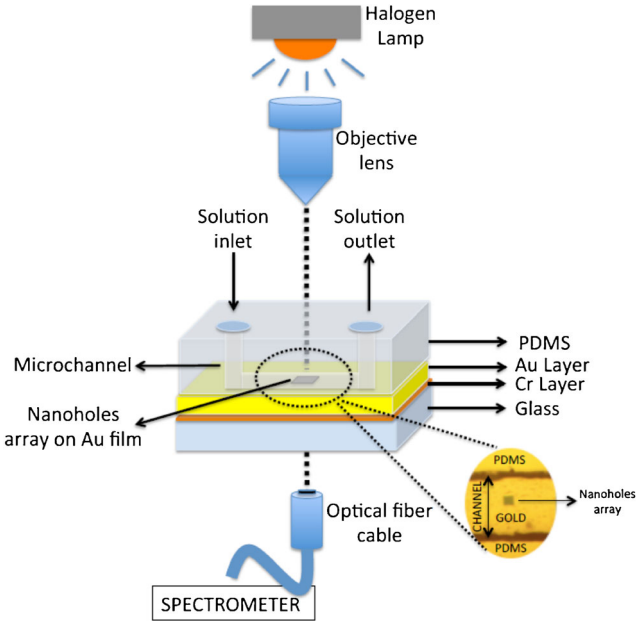

Fig. 1 Experimental optical arrangement integrated with microfluidic system in collinear transmission mode to obtain spectra of transmission across substrates that contain nanohole arrays on gold film. *Inset*: photographic image that shows the alignment of the PDMS microchannel with the array

the nanohole arrays in solutions with different refractive indices. For this purpose, aqueous solutions of D-(+)-glucose (Sigma, 99.5 %) at concentrations of 2.0, 6.0, 10.0, 14.0, 18.0, 22.0, 26.0, and 30.0 g 100 mL^{-1} were used. Each solution had its refractive index determined (with 0.0001 precision) by using a portable digital refractometer (Atago, 3850 PAL-RI).

Biosensing Analysis of HER2

An appropriate strategy was used to immobilize the molecular biorecognition element (antibody against HER2) on the metallic nanostructured surface. For gold surfaces, the immobilization is normally performed via streptavidin immobilized

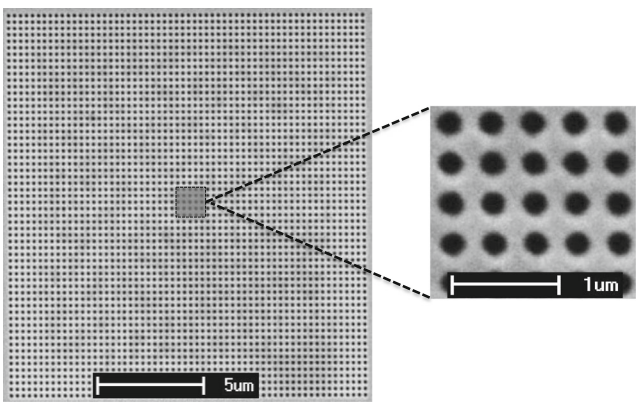

Fig. 2 SEM images at different magnifications of a square nanohole array on gold film with 400-nm periodicity, hole diameter of 200 nm, and depth of 105 nm (thickness)

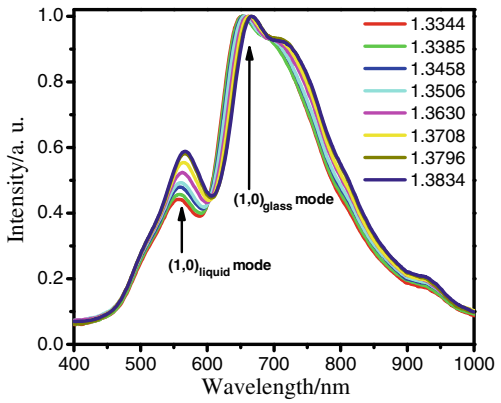

Fig. 3 Transmission spectra of nanohole arrays as a function of the refractive index (1.3344 to 1.3834). Array has a periodicity of 400 nm, and the hole diameter is 200 nm. The *bands* represent the $(1,0)_{liquid}$ and $(1,0)_{glass}$ plasmonic modes related to gold/liquid and gold/glass interfaces, respectively

previously on biotin [49–51]; in turn, the biotin is attached to the surface via covalent interaction by using an alkanethiol organized monolayer on the gold surface [52].

The surface with the biorecognizing element that would be received was prepared initially by immersing the nanohole arrays in an ultrasonic ethanolic bath for 5 min. Soon after, it was extensively rinsed with water and dried with N_2, and then, it was integrated with the microfluidic system. Subsequently, an aqueous solution of cysteamine (Aldrich 95 %) 0.06 mol L^{-1} was flowed on the substrate surface for 72 h. Afterwards, a 5-mg mL^{-1} aqueous solution of biotin-sulfo-NHS (Sigma-Aldrich, 90 %) was injected for 12 h. Then, 0.5 mg mL^{-1} of streptavidin in phosphate buffer solution (PBS, pH=7.4) was passed for 4 h.

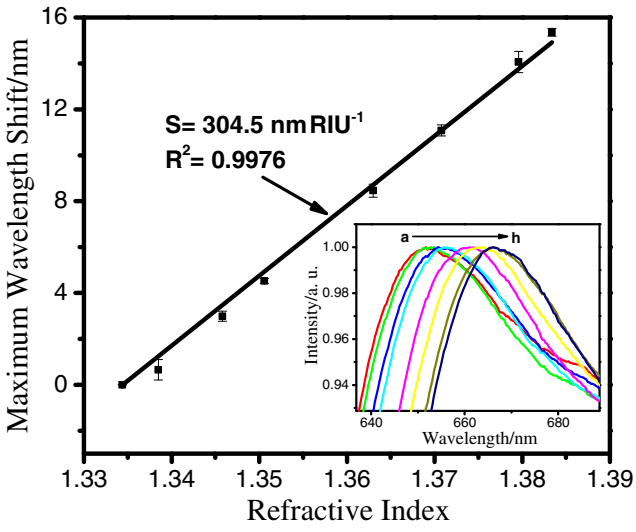

Fig. 4 Curve of λ_{max} shift as a function of refractive index for bands relating to $(1,0)_{glass}$ mode. The *inset* shows the $(1,0)_{glass}$ bands (expanded and normalized) for each refractive index tested. In the "a" to "h" range, the refractive index changes from 1.3344 to 1.3834

The previously prepared substrate was then modified by immobilization of biotinylated antibody against HER2 (AB1, Invitrogen, 95 %) via specific interaction with the previously immobilized streptavidin. This AB1 immobilization step was achieved by flowing a 50-μL mL^{-1} AB1 solution for 12 h. Soon after, a bovine serum albumin (BSA) solution (100 ng mL^{-1}) was flowed on the substrate for 2 h. This last step was necessary to block nonspecific binding sites. Finally, the HER2 antigen (Invitrogen, 70 %) was flowed on the substrate surface (already containing the antibody) by using a 30-ng mL^{-1} antigen solution for 1 h. To use the sandwich detection mode, a 5-μg mL^{-1} solution of a secondary antibody against HER2 (AB2, Invitrogen 75 mg L^{-1}) was flowed on the system for 2 h. The antibodies, the BSA, and the antigens were diluted in PBS.

After each modification step, the system was purged at a flow rate of 2 mL h^{-1} with PBS to remove loosely adsorbed molecules and the transmission spectra acquired. The flow rate of the successive modifications was 0.05 mL h^{-1}.

Results and Discussion

The square gold nanohole arrays constructed by FIB had a periodicity of 400 nm and a hole diameter of 200 nm with an active area of ca. 14×14 μm, as shown in Fig. 2.

Figure 3 shows the transmission spectra of the nanohole arrays immersed in glucose solutions of different refractive indices. Two bands were observed, and both undergo redshift as the refractive index increases, which is an expected behavior for plasmonic substrates [4, 53]. According to Eq. 1, the two bands are both related to the (1,0) modes for metal/liquid ($(1,0)_{liquid}$ mode) and metal/glass ($(1,0)_{glass}$ mode) interfaces, respectively. The λ_{max} is the maximum wavelength of the

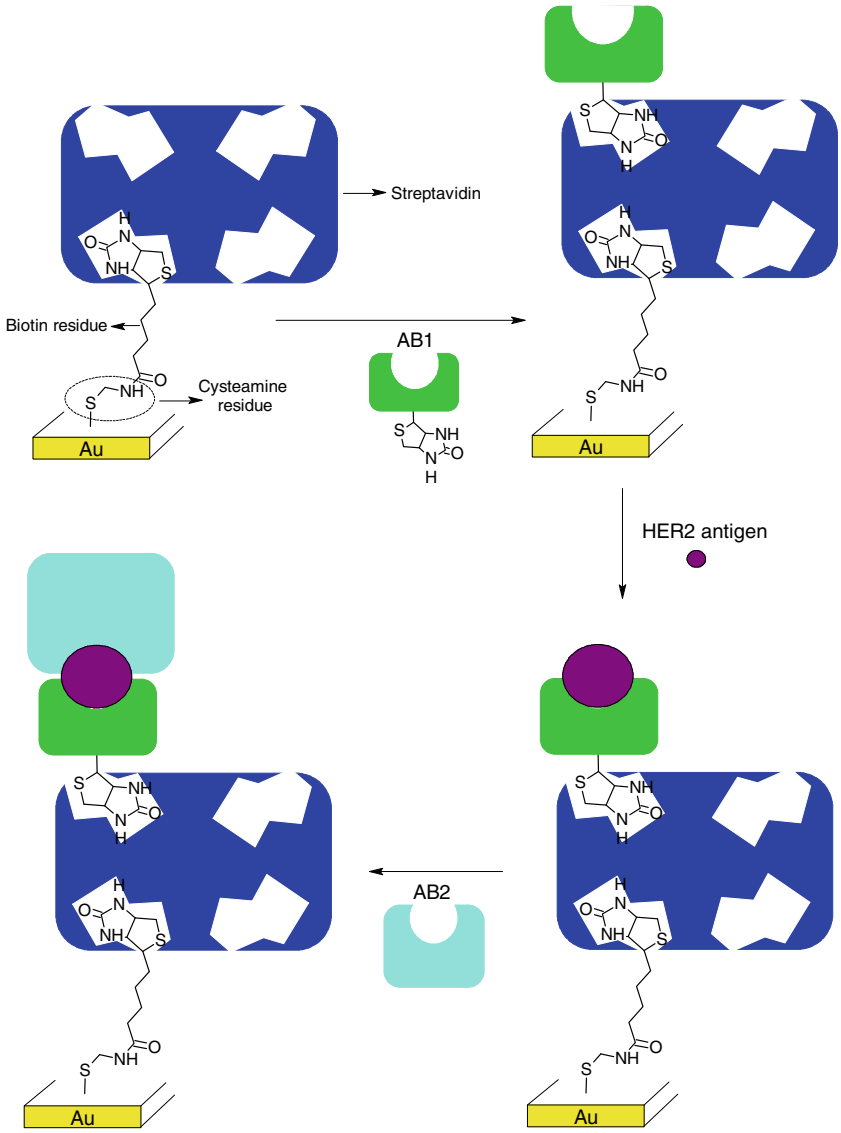

Fig. 5 Scheme of HER2 antigen detection via immobilized biotinylated antibody (AB1), starting from a metal surface that was previously prepared through a cysteamine streptavidin-biotin process. For the sandwich detection mode, a secondary antibody (AB2) was used

plasmon, a_0 is the periodicity of the array, i and j are integers relative to the plasmonic modes, and ε_d and ε_m are the dielectric constants of the dielectric materials ($\varepsilon_{glass} = 2.13$ and $\varepsilon_{liquid} = 1.78$, in the oscillation frequency for visible light) and metal (ε_{Au} depends on the wavelength and can be obtained elsewhere [54]), respectively.

$$\lambda_{max} = \frac{\alpha_0}{\sqrt{i^2 + j^2}} \sqrt{\frac{\varepsilon_d \varepsilon_m}{\varepsilon_d + \varepsilon_m}} \quad (1)$$

The $(1,0)_{glass}$ band possesses a higher sensitivity since the transmission maximum wavelength (λ_{max}) shifts, at the same solutions, are higher for this plasmonic mode. As can be seen in Fig. 3, a redshift of ca. 9 nm was obtained for the $(1,0)_{liquid}$ mode, while for the $(1,0)_{glass}$ mode, the redshift was ca. 15 nm when the refractive index changed from 1.3344 to 1.3834.

Since the plasmonic $(1,0)_{glass}$ mode show a higher sensitivity, the λ_{max} for that band was plotted as a function of the refractive index. The resultant curve slope (Fig. 4) is defined as the sensitivity of the plasmonic substrate, and its characterization is important in determining the ability of the substrate to have its plasmonic transmission band disturbed due to changes in refractive indexes on the metal surface [55]. The sensitivity obtained was ca. 305 nm RIU-1 (RIU=refractive index units) and is comparable to results reported in the literature for plasmonic devices of the same nature [5, 6]. It was also observed that there was a good linear fit since the linear fit coefficient (R^2) value was near unity (R^2=0.9976). It must be considered that a proportional response to the variation of refractive index is a sought parameter for SPR sensors. The inset of Fig. 4 shows the $(1,0)_{glass}$ region (magnified and normalized) obtained for each refractive index, which shows the redshift as the refractive index increased.

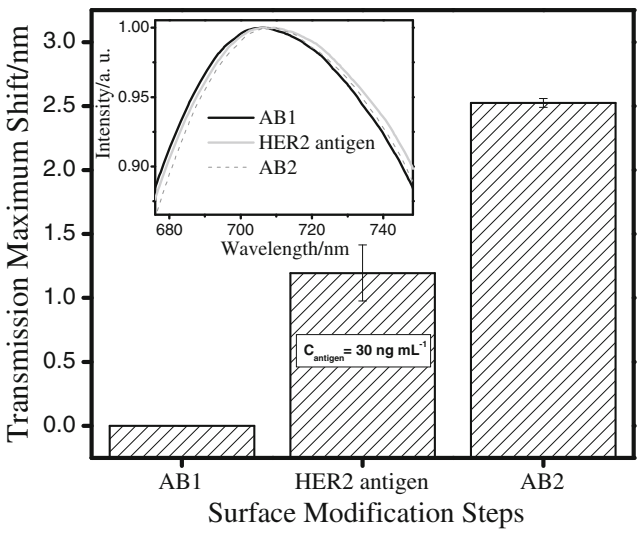

Fig. 6 The maximum wavelength shift (λ_{max}) for the $(1,0)_{glass}$ mode as a function of the metallic surface modification steps. The AB1 antibody immobilization was taken as zero, and the HER2 antigen concentration detected was 30 ng mL^{-1}. *Inset*: normalized and expanded transmission $(1,0)_{glass}$ band spectra for each modification step

Considering that the sensor proved to be able to detect variations in refractive indexes near the metallic surface, we used the sensor to test the detection of HER2, an antigen associated with breast cancer. For this, the nanohole gold surface was initially prepared by immobilization of a cysteamine monolayer and thereafter with biotin and streptavidin.

For the detection of the HER2 antigen, the surface received the AB1 molecules (biotinylated antibody) through its interaction with previously immobilized streptavidin molecules. Then, the HER2 antigen was immobilized, and finally, the surface received the AB2 antigen. The use of a secondary antibody, which characterizes the sandwich detection mode, improved the sensitivity of the sensor [3]; the antigens are molecules of relatively low molecular mass (small volume), which does not produce significant changes in refractive index. It is often difficult to detect the antigen by spectral monitoring. However, antigen conjugated with bulky secondary antibody causes a relatively larger change in the refractive index of the metal, which is then more easily detected through a spectral band shift. The surface modification scheme (starting from surface prepared with the cysteamine-biotin-streptavidin) is shown schematically in Fig. 5.

Figure 6 shows the transmission band shift for the $(1,0)_{glass}$ mode during the steps of the HER2 antigen detection (starting from AB1 immobilization).

The spectral shift observed for the $(1,0)_{glass}$ band (Fig. 6) is expected. As the molecules are immobilized on the surface, the refractive index on the metal/dielectric interface increases, leading to a redshift. Compared to the AB1 immobilization step, a shift of ca. 1.2 nm was observed when the HER2 antigen (concentration 30 ng mL^{-1}) was immobilized. An extra redshift of ca. 1.3 nm was observed when AB2 was linked to the AB1/HER2 layer; this resulted in a 2.5-nm total band displacement. This shift is comparable with those obtained in other studies that report the use of sensors based on nanohole arrays applied in biomolecular detection [56, 57]. Furthermore, considering that the transmission maximum shift obtained for the immobilization of AB2 was of 2.50± 0.03 nm (with respect to surface covered with AB1) and the fact that our system is capable of measurements with an accuracy of 0.1 nm, the signal-to-noise ratio is high enough so that the sensor can be efficiently used to detect HER2 antigen (in the tested concentration) and the observed shift is easily measured by our system.

We observed that the shifts regarding the immobilization of HER2 and AB2 are similar (1.2 and 1.3 nm, respectively). However, AB2 molecules are larger than the HER2 ones, which should imply a higher plasmonic-disturbing effect, but this was not observed. This possibly occurs because the SPs are confined on the metal surface, and the amplitude of the plasmon electromagnetic field (and hence sensitivity)

decays exponentially as it moves away from the metal/dielectric interface [58]. Thus, the AB2 molecules cause a smaller plasmonic perturbation than expected because they are relatively farther away from the surface (regarding the antigen molecules). Nevertheless, the sandwich detection mode clearly provided a greater sensitivity to the presence of biomolecules on the metal surface.

Conclusion

The nanohole array-based microfluidic sensor presented in this work was sensitive to the presence of the breast cancer biomarker at a concentration of 30 ng mL^{-1}. It is noteworthy that HER2-positive individuals have concentrations between 15 and 75 ng mL^{-1} in blood plasma [59]. Thus, the sensor shows potential to be applied in the diagnosis or prognosis of breast cancer. It is interesting to note that the SPR substrate showed good sensitivity (ca. 302 nm RIU^{-1}) and a great linear behavior when compared to other nanohole array-based plasmonic biosensors for spectral investigation.

Acknowledgments J. P. Monteiro thanks CAPES for the fellowship. We gratefully acknowledge Fundação Araucária (process no. 209/2014) and CNPq (process no. 473213/2011-7) for financial support.

References

1. Ebbesen TW, Lezec HJ, Ghaemi HF, Thio T, Wolff PA (1998) Extraordinary optical transmission through sub-wavelength hole arrays. Nature 391:667–669. doi:10.1038/35570
2. Bethe HA (1944) Theory of diffraction by small holes. Phys Rev 66:163–182. doi:10.1103/PhysRev.66.163
3. Homola J (2008) Surface plasmon resonance sensors for detection of chemical and biological species. Chem Rev (Washington, DC, U S) 108:462–493. doi:10.1021/cr068107d
4. De Leebeeck A, Kumar LKS, De Lange V, Sinton D, Gordon R, Brolo AG (2007) On-chip surface-based detection with nanohole arrays. Anal Chem 79:4094–4100. doi:10.1021/ac070001a
5. Gordon R, Sinton D, Kavanagh KL, Brolo AG (2008) A new generation of sensors based on extraordinary optical transmission. Acc Chem Res 41:1049–1057. doi:10.1021/ar800074d
6. Monteiro JP, Carneiro LB, Rahman MM, Brolo AG, Santos MJL, Ferreira J, Girotto EM (2013) Effect of periodicity on the performance of surface plasmon resonance sensors based on subwavelength nanohole arrays. Sensors Actuators B 178:366–370. doi:10.1016/j.snb.2012.12.090
7. Yanga JC, Ji J, Hoglea JM, Larson DN (2009) Multiplexed plasmonic sensing based on small-dimension nanohole arrays and intensity interrogation. Biosens Bioelectron 24:2334–2338. doi:10.1016/j.bios.2008.12.011
8. Tellez GAC, Ahmed A, Gordon R (2012) Optimizing the resolution of nanohole arrays in metal films for refractive-index sensing. Appl Phys A Mater Sci Process 109:775–780. doi:10.1007/s00339-012-7405-5
9. Kretschmann E, Raether HZ (1968) Radiative decay of nonradiative surface plasmons excited by light Z. Naturforsch 23A 23:2135–2136. doi: citeulike-article-id:3901347
10. Patel PDJ (2006) Overview of affinity biosensors in food analysis. J AOAC Int 89:805
11. Lazcka O, Campo FJD, Munoz FX (2007) Pathogen detection: a perspective of traditional methods and biosensors. Biosens Bioelectron 22:1205–1217. doi:10.1016/j.bios.2006.06.036
12. Leonard P, Hearty S, Brennan J, Dunne L, Quinn J, Chakraborty T, O'Kennedy R (2003) Advances in biosensors for detection of pathogens in food and water. Enzym Microb Technol 32:3–13. doi:10.1016/S0141-0229(02)00232-6
13. Mello LD, Kubota LT (2002) Review of the use of biosensors as analytical tools in the food and drink industries. Food Chem 77:237–256. doi:10.1016/S0308-8146(02)00104-8
14. Baeumner AJ (2003) Biosensors for environmental pollutants and food contaminants. Anal Bioanal Chem 377:434–445. doi:10.1007/s00216-003-2158-9
15. Farre M, Martinez E, Ramon J, Navarro A, Radjenovic J, Mauriz E, Lechuga L, Marco MP, Barcelo D (2007) Part per trillion determination of atrazine in natural water samples by a surface plasmon resonance immunosensor. Anal Bioanal Chem 388:207–214. doi:10.1007/s00216-007-1214-2
16. Shankaran DR, Matsumoto K, Toko K, Miura N (2006) Performance evaluation and comparison of four SPR immunoassays for rapid and label-free detection of TNT. Electrochemistry (Tokyo, Jpn) 74:141–144. doi:10.5796/electrochemistry.74.141
17. Kim SJ, Gobi KV, Harada R, Shankaran DR, Miura N (2006) Miniaturized portable surface plasmon resonance immunosensor applicable for onsite detection of low-molecular-weight analytes. Sensors Actuators B 115:349–256. doi:10.1016/j.snb.2005.09.025
18. Ock K, Jang G, Roh Y, Kim S, Kim J, Koh K (2001) Optical detection of Cu2+ ion using a SQ-dye containing polymeric thin-film on Au surface. Microchem J 70:301–305. doi:10.1016/S0026-265X(01)00133-3
19. Soh N, Watanabe T, Asano Y, Imato T (2003) Indirect competitive immunoassay for bisphenol A based on a surface plasmon resonance sensor. Sens and Materials 15:423–438
20. Soh N, Tokuda T, Watanabe T, Mishima K, Imato T, Masadome T, Asano Y, Okutani S, Niwa O, Brown S (2003) A surface plasmon resonance immunosensor for detecting a dioxin precursor using a gold binding polypeptide. Talanta 60:733–745. doi:10.1016/S0039-9140(03)00139-5
21. Shimomura M, Nomura Y, Zhang W, Sakino M, Lee KH, Ikebukuro K, Karube I (2001) Simple and rapid detection method using surface plasmon resonance for dioxins, polychlorinated biphenylx and atrazine. Anal Chim Acta 434:223–230. doi:10.1016/S0003-2670(01)00809-1
22. Gobi KV, Iwasaka H, Miura N (2007) Self-assembled PEG monolayer based SPR immunosensor for label-free detection of insulin. Biosens Bioelectron 22:1382–1389. doi:10.1016/j.bios.2006.06.012
23. Dillon PP, Daly SJ, Manning BM, O'Kennedy R (2003) Immunoassay for the determination of morphine-3-glucuronide using a surface plasmon resonance-based biosensor. Biosens Bioelectron 18:217–227. doi:10.1016/S0956-5663(02)00182-3
24. Fitzpatrick B, O'Kennedy R (2004) The development and application of a surface plasmon resonance-based inhibition immunoassay for the determination of warfarin in plasma ultrafiltrate. J Immunol Methods 291:11–25. doi:10.1016/j.jim.2004.03.015
25. Ladd J, Boozer C, Yu Q, Chen S, Homola J, Jiang S (2004) DNA-directed protein immobilization on mixed self-assembled monolayers via a streptavidin bridge. Langmuir 20:8090–8095. doi:10.1021/la049867r
26. Chung JW, Bernhardt R, Pyun JC (2006) Sequential analysis of multiple analytes using a surface plasmon resonance (SPR) biosensor. J Immunol Methods 311:178–188. doi:10.1016/j.jim.2006.02.003

27. Miyashita M, Shimada T, Miyagawa H, Akamatsu M (2005) Surface plasmon resonance-based immunoassay for 17beta-estradiol and its application to the measurement of estrogen receptor-binding activity. Anal Bioanal Chem 381:667–673. doi:10.1007/s00216-004-2952-z
28. Cao C, Kim JP, Kim BW, Chae H, Yoon HC, Yang SS, Sim SJ (2006) A strategy for sensitivity and specificity enhancements in prostate specific antigen-alpha1-antichymotrypsin detection based on surface plasmon resonance. Biosens Bioelectron 21:2106–2113. doi:10.1016/j.bios.2005.10.014
29. Li Y, Lee HJ, Corn RM (2007) Detection of protein biomarkers using RNA aptamer microarrays and enzymatically amplified surface plasmon resonance imaging. Anal Chem (Washington, DC, U S) 79:1082–1088. doi:10.1021/ac061849m
30. Besselink GA, Kooyman RP, van Os PJ, Engbers GH, Schasfoort RB (2004) Signal amplification on planar and gel-type sensor surfaces in surface plasmon resonance-based detection of prostate-specific antigen. Anal Biochem 333:165–173. doi:10.1016/j.ab.2004.05.009
31. Wu LP, Li YF, Huang CZ, Zhang Q (2006) Visual detection of Sudan dyes based on the plasmon resonance light scattering signals of silver nanoparticles. Anal Chem 78:5570–5577. doi:10.1021/ac0603577
32. Chung JW, Bernhardt R, Pyun JC (2006) Additive assay of cancer marker CA 19-9 by SPR biosensor. Sensors Actuators B 118:28–32. doi:10.1016/j.snb.2006.04.015
33. Yang CY, Brooks E, Li Y, Denny P, Ho CM, Qi FX, Shi WY, Wolinsky L, Wu B, Wong DTW, Montemagno CD (2005) Detection of picomolar levels of interleukin-8 in human saliva by SPR. Lab Chip 5:1017–1023. doi:10.1039/b504737d
34. Tang DP, Yuan R, Chai YQ (2006) Novel immunoassay for carcinoembryonic antigen based on protein A-conjugated immunosensor chip by surface plasmon resonance and cyclic voltammetry. Bioprocess Biosyst Eng 28:315–321. doi:10.1007/s00449-005-0036-x
35. Monfregola L, Vitale RM, Amodeo P, De Luca S (2009) A SPR strategy for high-throughput ligand screenings based on synthetic peptides mimicking a selected subdomain of the target protein: a proof of concept on HER2 receptor. Bioorg Med Chem 17:7015–7020. doi:10.1016/j.bmc.2009.08.004
36. Hunta HK, Armani AM (2010) Label-free biological and chemical sensors. Nanoscale 2:1544–1559. doi:10.1039/c0nr00201a
37. Escobedo C, Brolo AG, Gordon R, Sinton D (2010) Flow-through vs flow-over: analysis of transport and binding in nanohole array plasmonic biosensors. Anal Chem 82:10015–10020. doi:10.1021/ac101654f
38. Ji J, O'Connell JG, Carter DJD, Larson DN (2008) High-throughput nanohole array based system to monitor multiple binding events in real time. Anal Chem 80:2491–2498. doi:10.1021/ac7023206
39. Eftekhari F, Escobedo C, Ferreira J, Duan X, Girotto EM, Brolo AG, Gordon R, Sinton D (2009) Nanoholes as nanochannels: flow-through plasmonic sensing. Anal Chem 81:4308–4311. doi:10.1021/ac900221y
40. Escobedo C, Chou Y-W, Rahman M, Duan X, Gordon R, Sinton D, Brolo AG, Ferreira J (2013) Quantification of ovarian cancer markers with integrated microfluidic concentration gradient and imaging nanohole surface plasmon resonance. Analyst 138:1450–1458. doi:10.1039/c3an36616b
41. Basil CF, Zhao YD, Zavaglia K, Jin P, Panelli MC, Voiculescu S, Mandruzzato S, Lee HM, Seliger B, Freedman RS, Taylor PR, Hu N, Zanovello P, Marincola FM, Wang E (2006) Common cancer biomarkers. Cancer Res 66:2953–2961. doi:10.1158/0008-5472.CAN-05-3433
42. Esteva FJ, Cheli CD, Fritsche H, Fornier M, Slamon D, Thiel RP, Luftner D, Ghani F (2005) Clinical utility of serum HER2/neu in monitoring and prediction of progression-free survival in metastatic breast cancer patients treated with trastuzumab-based therapies. Breast Cancer Res 7:R436–R443. doi:10.1186/bcr1020
43. Coussens L, Yang-Feng TL, Lioa YC, Chen E, Gray A, McGrath J, Seeburg PH, Libermann TA, Schlessinger J, Francke U, Levinson A, Ullrich A (1985) Tyrosine kinase receptor with extensive homology to EGF receptor shares chromosomal location with neu oncogene. Science 230:1132–1139. doi:10.1126/science.2999974
44. Schecter AL, Stern DF, Vaidyanathan L, Decker SJ, Drebin JA, Greene MI, Weinberg AR (1984) The neu oncogene: an erb-B-related gene encoding a 185,000-Mr tumour antigen. Nature 312:513–516. doi:10.1038/312513a0
45. Slamon DJ, Goldolphin W, Jones LA, Holt JA, Wong SG, Keith DE, Levin WJ, Stuart SG, Udove J, Ullrich A (1989) Studies of the HER-2/neu proto-oncogene in human breast and ovarian cancer. Science 244:707–712. doi:10.1126/science.2470152
46. Gown AM (2008) Current issues in ER and HER2 testing by IHC in breast cancer. Mod Pathol 21:S8–S15. doi:10.1038/modpathol.2008.34
47. Freitas CS (2008) Estendendo o Conhecimento sobre a Família Her-Receptores para o Fator de Crescimento Epidérmico e seus ligantes às Malignidades Hematológicas. Revista Brasileira de Cancerologia 54:79–86
48. Carneiro LB, Ferreira J, Santos MJL, Monteiro JP, Girotto EM (2011) A new approach to immobilize poly (vinyl alcohol) on poly (dimethylsiloxane) resulting in low protein adsorption. Appl Surf Sci 257:10514–10519. doi:10.1016/j.apsusc.2011.07.031
49. Huang NP, Voros J, De Paul SM, Textor M, Spencer ND (2002) Biotin-derivatized poly (L-lysine)-g-poly (ethylene glycol): a novel polymeric interface for bioaffinity sensing. Langmuir 18:220–230. doi:10.1021/la010913m
50. Marie E, Dahlin AB, Tegenfeldt JO, Hook F (2007) Generic surface modification strategy for sensing applications based on AuSiO2 nanostructures. Biointerphases 2:49–55. doi:10.1116/1.2717926
51. Fei X, Guoliang Z, Marcus T, Wolfgang K (2006) Surface plasmon optical detection of beta-lactamase binding to different interfacial matrices combined with fiber optic absorbance spectroscopy for enzymatic activity assays. Biointerphases 1:73–81. doi:10.1116/1.2219109
52. Knoll W, Liley M, Piscevic D, Spinke J, Tarlov MJ (1997) Supramolecular architectures for the functionalization of solid surfaces. Adv Biophys 34:231–251. doi:10.1016/S0065-227X(97)89642-6
53. Homola J, Yee SS, Gauglitz G (1999) Surface plasmon resonance sensors: review. Sensors Actuators B 54:3–15. doi:10.1016/S0925-4005(98)00321-9
54. Novotny L, Hecht B (2006) Principles of nano-optics. Cambridge University Press, Cambridge
55. Pang L, Hwang GM, Slutsky B, Fainman Y (2007) Spectral sensitivity of two-dimensional nanohole array surface plasmon polariton resonance sensor. Appl Phys Lett 91:123112. doi:10.1063/1.2789181
56. Eftekhari F, Escobedo C, Ferreira J, Duan X, Girotto EM, Brolo AG, Gordon R, Sinton D (2009) Nanoholes as nanochannels: flow-through plasmonic sensing. Anal Chem 81:4308–4311. doi:10.1021/ac900221y
57. Im H, Shao H, Park YI, Peterson VM, Castro CM, Weissleder R, Lee H (2014) Label-free detection and molecular profiling of exosomes with a nano-plasmonic sensor. Nat Biotechnol 32:490–498. doi:10.1038/nbt.2886
58. Zayats AV, Smolyaninov II, Maradudin AA (2005) Nano-optics of surface plasmon polaritons. Phys Rep 408:131–314. doi:10.1016/j.physrep.2004.11.001
59. Meenakshi A, Kumar RS, Kumar NS (2002) ELISA for quantitation of serum C-erbB-2 oncoprotein in breast cancer patients. J Immunoassay Immunochem 23:293–305. doi:10.1081/IAS-120013028